7th Australasian Hydraulics and
Fluid Mechanics Conference,
Brisbane, 18-22 August, 1980

Wall Pressure Fluctuations in a Separated Region Downstream of a Corner

D.C. STEVENSON
Professor and Head of Department of Mechanical Engineering, The University of Canterbury, New Zealand
and
H.B. NUGYEN
Royal Institute of Technology, Stockholm

SUMMARY Measurements were made of the flow in a separated region downstream of a right angle bend in a duct for Reynolds numbers varying from 1.4×10^5 to 1.2×10^6. The effects, due to changes in upstream turbulence boundary layer thickness and minor changes of channel geometry, were measured. The extent of the separated region varied from 2.0 to 2.8 channel widths depending on the method of measurement, but there was no apparent effect due to Reynolds number. The peak wall pressure fluctuation occurred at the region of reattachment and could be 30 dB above that for an attached turbulent boundary layer.

1 INTRODUCTION

Turbulent boundary layers, jets and separated flow are all sources of aerodynamic noise. Although much experimental and theoretical work has been carried out on jet and turbulent boundary layer noise, as far as the authors are aware, relatively little has been published on noise generated by incompressible separated flows. Work on pressure fluctuations in a separated flow region due to a fence has been published by Fricke & Stevenson, and Emery & Mohsen. Pressure fluctuations in turbulent pipe flow due to a mitred bend have been investigated by Bull, who carried out both theoretical and experimental programmes. A number of workers have investigated turbulence and pressure fluctuations, in incompressible separated flows from steps, most being rearward facing.

The flow around curved bends has been studied and existence of secondary circulation was recognised as early as 1876 by Thompson. Considerable work has been carried out for both laminar and turbulent flows in curved pipes. Less has been done for sharp bends. Tunsdall & Harvey studied turbulent flow through a mitred right angled bend and more recently, Bull and Norton investigated noise due to a mitred bend in a circular pipe.

2 DESCRIPTION OF TEST SECTION

The low noise wind tunnel used is shown in Figure 1,

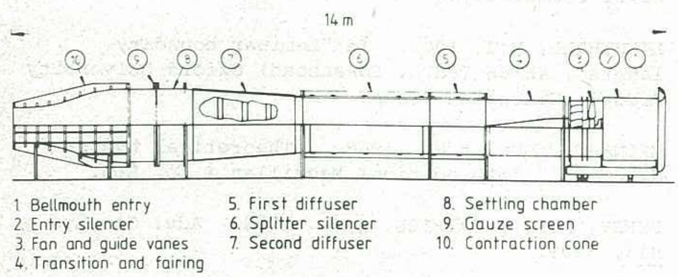

Figure 1 Low Noise Wind Tunnel

and the right angled bend at the end of the contraction is shown in Figure 2. An acoustic termination followed the test section to prevent reflection of sound from the exit and measurements showed that no standing waves were present. The test section was 0.76m x 0.76m and an internal vertical wall enabled the width of the test section to be varied. The entry section to the bend was 1.2m long to the inner wall and the exit section 1.96m to the acoustic termination. The acoustic termination was 0.6m long. The wind tunnel was fitted with both a dissipative splitter and a resonant type silencer and the noise level in the wind tunnel due to the wind tunnel drive was in the worst case, 8 dB below the minimum levels recorded in the test, but was usually much more than this. The velocity entering the upstream test section was within 1% of the mean velocity and the upstream turbulence measured from 0.25% to 0.45% depending on the velocity.

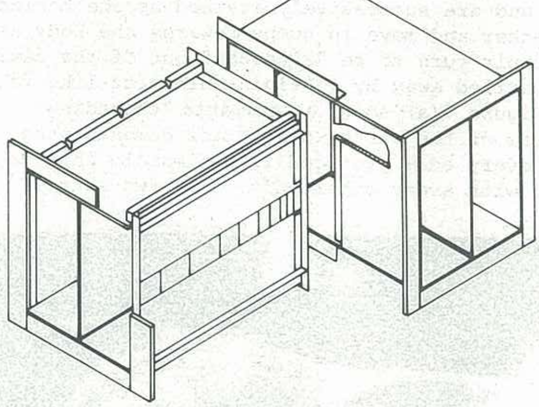

Figure 2 Right Angled Bend

Visualisation of the flow was also observed with the aid of dye injection in a .15m x .10m water duct with a right angled bend.

3 INSTRUMENTATION

For the static and total head pressure measurements, Betz micromanometers were used. The fluctuating surface pressure measurements were made using Brüel & Kjaer ½" microphones, spectrometer type 2112 and recorder type 2305. Unfortunately, frequencies below 20 Hz could not be analysed. Turbulence was measured using Disa hot wire probes type 55F31 and constant temperature anemometer unit 55D01 with a 55D10 lineariser. In addition to flow visualisation using dye in the water tunnel and wool tufts in the wind tunnel, the orifice dam technique of Roshko & Thomke was used to determine reattachment positions. The wedge used had a 30° wedge angle, was 6mm high and 6mm wide. With the wedge positioned upstream of the static pressure tapping (thin edge forward), a decrease in the static pressure is recorded.

4 RESULTS AND DISCUSSIONS

In order to investigate the effect of scale, three test sections, widths 0.25, 0.38 and 0.76, were used, and the velocity was varied between 8m/s and 22m/s for most tests. Thus the Reynolds number varied from 1.4×10^5 to 1.2×10^6. The Reynolds numbers for the test in the water tunnel varied from 4.1×10^3 to 2×10^4.

4.1 Flow Visualisation

At the lower speed (.03m/s) a distinct vortex shedding pattern was observed from the corner. When the flow velocity increased to .15m/s the vortex shedding was more rapid and the size of the vortices reduced, but the angle they left the corner was the same. For the velocities investigated the reattachment point was found downstream at approximately 2.7 channel widths of the tunnel.

Two distinct large vortices were observed near the top and bottom of the tunnel starting close to the far wall. They rotated in opposite directions and propagated downstream towards the reattachment region on the near wall.

The wool tufts used in the wind tunnel showed distinct directions of flow on either side of the reattachment region. Near the reattachment region the tufts changed direction continually indicating that any hot wire measurements under these conditions would be useless. Table I below includes the reattachment length to width ratio as determined by wool tufts in the wind tunnel. The static pressure distribution on the near wall downstream of the corner with and without orifice dams upstream of each pressure tapping was plotted. The curves crossed at x/w for 2.6 giving a reliable indication of the reattachment point.

TABLE I

Reattachment Length Xr/w

Section Width w	Water Tunnel	Wool Tufts	Orifice Dam	Pitot Static Tube	RMS Pressure Fluctuations
0.25m	-	2.5	2.6	2.8	2.2
0.38m	-	2.2	2.6	2.6	2.0
0.76m	-	2.0	-	2.2	1.8
0.15m	2.7	-	-	-	-

4.1.1 Mean velocity profiles

Mean velocity profiles for different tunnel widths and speeds were taken and as there was no significant difference between them, only one representative profile, w = .25m, is shown in Figure 3. The reference velocity U_o was measured upstream of the corner in the uniform approaching flow. The line of zero velocity was drawn by approximating the positions where the Pitot readings were zero. These positions were not easily determined since in their vicinity the Pitot static readings were very unsteady and often registered negative values. Inside the separation zone with the Pitot static tube pointing towards the tunnel exit, reverse flow velocities were read satisfactorily. The reattachment position was determined by extrapolation of the zero velocity line and is given in Table I for the different tunnel widths. In Figure 3, the locus of the inflection points of the velocity profiles is labelled $\overline{u'v'}_{max}$. The values were not measured but the line was drawn according to the results of Emery & Mohsen.

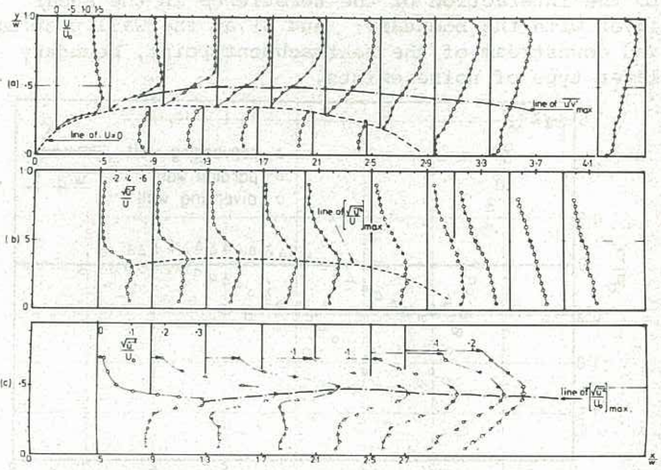

Figure 3 Mean Velocity and Turbulence Profiles

4.2 Turbulence Intensity Measurement

The values of $u'/\bar{U}$ are also shown in Figure 3 but would be erroneous near the dotted line. Nonetheless the line of $u'/\bar{U}_{max}$ agrees well with the line u = 0 in the velocity profile curve.

4.3 Mean Wall Static Pressure

The shapes of the wall static distributions were approximately the same for different speeds and tunnel widths. On the near wall the pressure immediately behind the corner is negative and becomes more so with distance of about one section width, and then rises rapidly (see Figure 4). Not unexpectedly, on the far wall a region of positive pressure up to 1.4 tunnel widths was observed. The pressure then dropped rapidly indicating a possible separation on this wall and then rises rapidly in almost the same way as the near wall. There was only a small difference in pressure distribution between the widths of the section. For approximately five tunnel widths downstream of the corner both sides are under negative pressure.

4.3.1 Variation of static pressure with upstream boundary layer thickness and turbulence

The boundary layer upstream of the corner was thickened by 12.5mm wooden cubes. This gave rise to a slight pressure increase on the inner wall immediately behind the corner, but elsewhere there was no change.

A square mesh grid of .8mm wire diameter and 18mm spacing was placed across the entry section 300mm ahead of the corner. There was a very small rise in the static pressure in the near wall immediately behind the corner. Unfortunately, it was not possible to develop a very thick boundary layer upstream of the corner to investigate, say, the effect of fully developed pipe flow.

4.3.2 Converging and diverging walls

When the far wall was inclined 1.5° to form both diverging and converging sections, the static pressure distribution was significantly modified as shown in Figure 4.

4.4 Fluctuating Wall Pressures

In the flow around the corner, there are three main sources of noise generation: 1) noise radiated from the turbulent shear layer from the edge of the corner which is analogous to the turbulent mixing region of a jet; 2) in the vicinity of reattachment point, a dipole type of noise is generated due to the interaction of the turbulence in the shear layer with the boundary; and 3) at the wall upstream and downstream of the reattachment point, boundary layer type of noise exists.

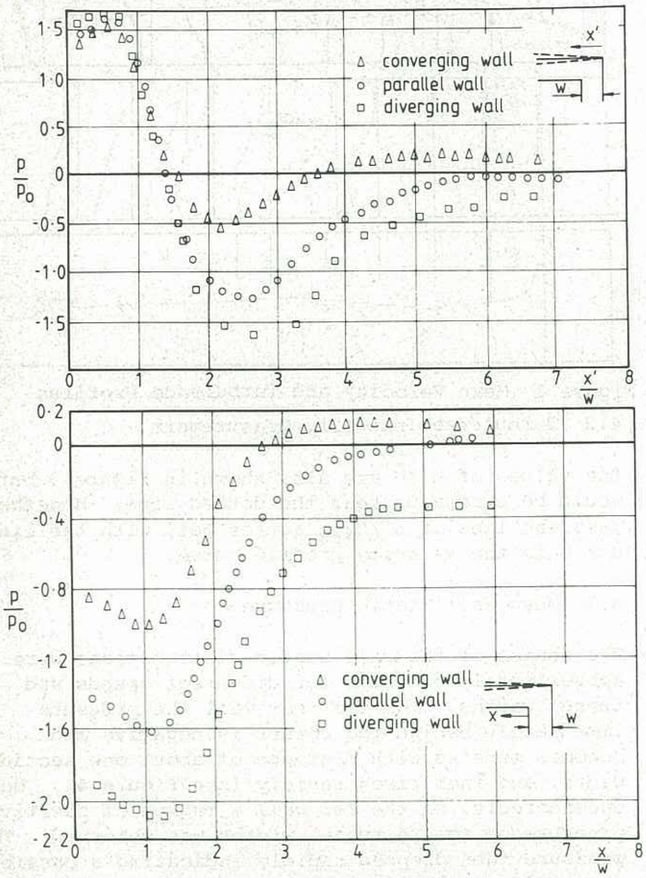

Figure 4 Mean Wall Static Pressures and Effect of Converging and Diverging Sections

The minimum sound pressure level in the separated flow for an upstream velocity of 16.5m/s was 112 dB. This means that the noise measured on the wall was contributed mostly from the outside flow and not from the reverse flow in the separated region which would give approximately 82 dB assuming $p'/q_o = .006$ for normal attached turbulent boundary layers.

4.4.1 Effect of flow velocity

Figure 5 shows the variation of p'/q_o with x/w for three flow velocities. Near the reattachment region there is a broad peak with a level of p'/q_o in excess of 0.20, which corresponds to 124 dB or more than 30 dB above the pseudo boundary layer noise in a turbulent boundary layer at the same flow velocity. Near the corner the level recorded is most likely to be due to the quadropole noise in the turbulent

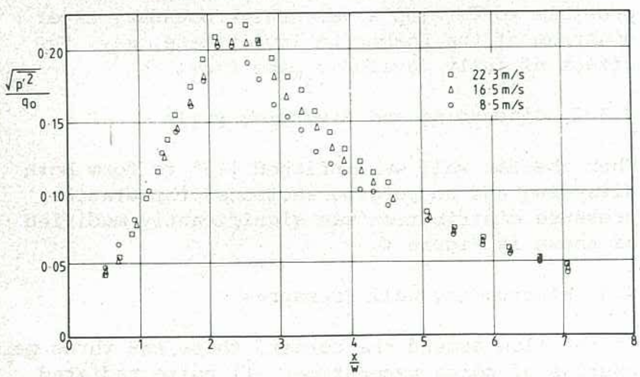

Figure 5 Wall Pressure Fluctuations: Effect of Flow Velocity

shear layer. Further downstream the level increases indicating contributions from other sources with the peak near the reattachment region. The peaks were quite broad indicating a wide region of reattachment. Downstream the level reduced slowly to the level at the corner at about seven section widths.

4.4.2 Effect of tunnel width

Figure 6 shows that when the test section width is increased the reattachment length, as determined by the maximum root mean square pressure fluctuation, is reduced which is in general agreement with other measurements (see Table I). However, the results for a tunnel width of 0.76m do not agree at all well with the other two tunnel widths. Near the corner the value of p'/q_o is much higher and this may be due to low frequency parasitic noise that was below the limit of the frequency analyser available (down to 20 Hz) but not when the total signal was being recorded (down to 2 Hz). For larger x/w the curve is also in disagreement and this could be the influence of the tunnel exit which was much closer to the reattachment point for the tunnel width of 0.76m.

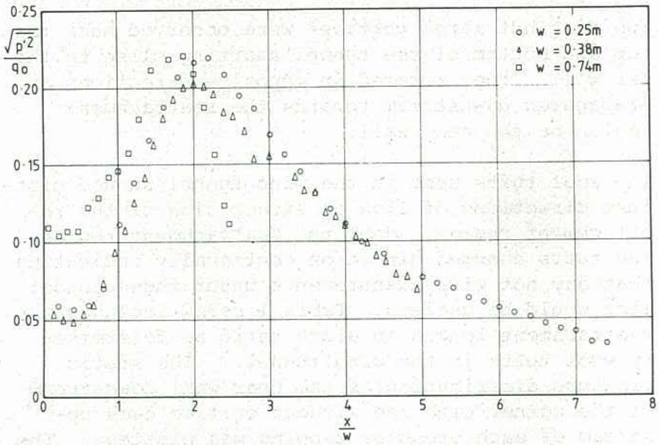

Figure 6 Wall Pressure Fluctuations : Effect of Tunnel Width

It is also possible that the effect of secondary flows may be more pronounced with the wider section since it was square and had a much lower height to width ratio.

4.4.3 Effect of upstream boundary layer thickness and turbulence

For the changes in boundary layer thickness and turbulence induced (see 4.3.1) there was little change in p'/q_o at U_o = 16.5m/s.

4.4.4 Converging and diverging walls

Figure 7 shows the variation of p'/q_o with wall inclination indicating that the noise level and reattachment length are reduced with a favourable pressure gradient and conversely for the diverging wall.

4.4.5 Effect of corner radius

Three corner radii were used, namely 0, 6mm and 13mm. The variation of p'/q_o was essentially unchanged except that the peak at x/w = 2.5 was reduced by about 10% for the sharp corner and was about the same for both other radii.

4.5 Power Spectra of the Wall Pressure Fluctuations

Figure 8 shows the variation of power spectra with distance from the corner. Immediately behind the corner (x/w = 0.5) there is much more energy at low frequencies than in the attached layer upstream of the corner (x/w = -1.2). In the reattachment region (x/w = 2.5) the spectrum has the highest values at all frequencies and further downstream the levels decrease slowly. For variation in velocity from 11.6m/s to 19.5m/s the spectra measured at x/w = 0.5 showed no variation within experimental accuracy. For variation in section width the spectra for w = 0.38m and 0.76m were below those for w = 0.25m over most of the range. When lower frequencies were reached ($\omega\delta^*/U_o = 2 \times 10^{-2}$) the spectral densities for the three different widths were the same. For variation of upstream roughness and turbulence there was no change in the spectrum for x/w = 0.9, 2.5 and 4.1. For corner radii of 0, 6mm and 13mm, the spectrum for the sharp corner was lower than the other two radii which had approximately the same value. This difference increased with increasing frequency.

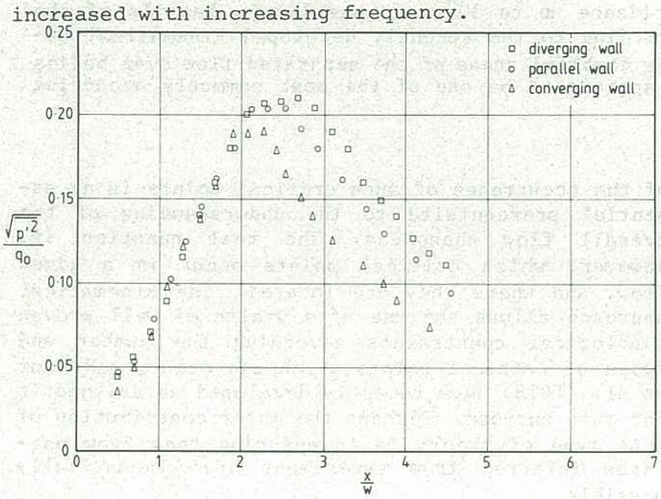

Figure 7 Wall Pressure Fluctuations : Effect of Converging and Diverging Walls

5 CONCLUSIONS

Table I shows the extent of the separated region around a right angled corner for different methods of measurement.

The mean wall static pressure distributions were insensitive to the velocity and the limited changes of boundary layer thickness and turbulence introduced upstream; relatively insensitive to changes in section width, but sensitive to inclination of the far wall.

The RMS pressure distributions (pseudo-noise) showed a maximum at reattachment which was 30 dB above that of a normal attached turbulent boundary layer for the same external flow conditions. There was little effect of flow velocity or section width when the data was plotted in a non-dimensional form except that there were discrepancies for the largest width (0.76m) probably due to apparatus and analysing equipment deficiencies. There was little effect of the limited changes of upstream boundary layer thickness and turbulence but the effect of far wall inclination was quite marked. The peak level for a sharp corner is slightly less than that for a slightly rounded corner.

Power spectra were not sensitive to changes in velocity or the limited changes in upstream

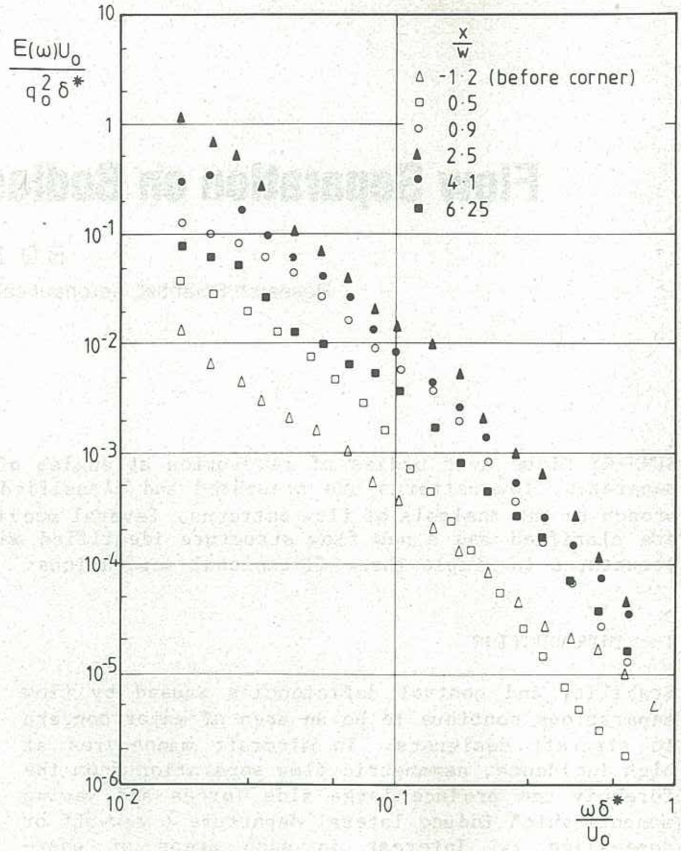

Figure 8 Power Spectra of the Wall Pressure Fluctuations

boundary layer thickness and turbulence.

6 REFERENCES

BULL, M.K. and NORTON, M.P. (1977), Pressure fluctuations in turbulent pipe flow due to a mitred bend. Proc.I.E. Aust.6th Australasian Hydraulics and Fluid Mechanics Conference, Adelaide, pp 273-77.

EMERY, A.F. and MOHSEN, A.M. (1968), An experimental study of the separated flow of very thick incompressible turbulent boundary layers, ASME, 68-WA/FE-36.

FRICKE, F.R. and STEVENSON, D.C., Pressure fluctuations in a separated flow region, J.A.S.A. vol.44, No.5, pp 1189-1200.

ROSHKO, A. and THOMKE, G.J. (1960), Observations of turbulent reattachment behind an axisymmetric downstream-facing step in supersonic flow, A.I.A.A. Journ., vol.4, No.6, pp 975-80.

THOMPSON, J., (1876), On the origin of windings of rivers in alluvial plains with remarks on the flow of water round bends in pipe, Proc. Roy. Soc. vol.A25, pp5-8.

TUNSDALL, M.J. and HARVEY, J.K. (1968), On the effect of a sharp bend in a fully developed turbulent pipe flow, J. Fl. Mech., vol.34(3), pp 585-609.